

Number counts and clustering properties of bright Distant Red Galaxies in the UKIDSS Ultra Deep Survey Early Data Release

S. Foucaud^{1*}, O. Almaini¹, I. Smail², C. J. Conselice¹, K. P. Lane¹, A. C. Edge²,
C. Simpson³, J. S. Dunlop⁴, R. J. McLure⁴, M. Cirasuolo⁴, P. Hirst⁵, M. G. Watson⁶,
and M. J. Page⁷

¹*School of Physics and Astronomy, University of Nottingham, University Park, Nottingham NG7 2RD*

²*Institute for Computational Cosmology, Department of Physics, Durham University, Durham DH1 3LE*

³*Astrophysics Research Institute, Liverpool John Moores University, Egerton Wharf, Birkenhead CH41 1LD*

⁴*SUPA† Institute for Astronomy, University of Edinburgh, Royal Observatory, Edinburgh EH9 3HJ*

⁵*Joint Astronomy Centre, 660 N. A’ohoku Place, University Park, Hilo, Hawaii 96720, U.S.A.*

⁶*X-ray Astronomy Group, Department of Physics and Astronomy, University of Leicester, Leicester LE1 7RH*

⁷*Mullard Space Science Laboratory, University College London, Gower Street, London WC1E 6BT*

Accepted ... Received ...; in original form ...

ABSTRACT

We describe the number counts and spatial distribution of 239 Distant Red Galaxies (DRGs), selected from the Early Data Release of the UKIDSS Ultra Deep Survey. The DRGs are identified by their very red infrared colours with $(J - K)_{AB} > 1.3$, selected over 0.62 deg^2 to a 90% completeness limit of $K_{AB} \simeq 20.7$. This is the first time a large sample of bright DRGs has been studied within a contiguous area, and we provide the first measurements of their number counts and clustering. The population shows strong angular clustering, intermediate between those of K -selected field galaxies and optical/infrared-selected Extremely Red Galaxies. Adopting the redshift distributions determined from other recent studies, we infer a high correlation length of $r_0 \sim 12 h^{-1} \text{ Mpc}$. Such strong clustering could imply that our galaxies are hosted by very massive dark matter halos, consistent with the progenitors of present-day $L \gtrsim L_*$ elliptical galaxies.

Key words: galaxies: high-redshift – cosmology: observations – galaxies: evolution.

1 INTRODUCTION

A new near-infrared selection technique has been developed in recent years to sample galaxies in the high-redshift Universe. By relying on purely near-infrared colours, this potentially avoids many biases which are inherent in optical techniques, particularly for detected dusty and/or evolved galaxies. Franx et al. (2003) argue that the simple $(J - K)_{AB} > 1.3$ colour selection criteria produces a sample that is mainly populated by galaxies at $z > 2$, at least at faint K -band magnitudes ($K_{AB} \gtrsim 21$). These are the so-called Distant Red Galaxies (hereafter DRGs). In the Faint Infrared Extragalactic Survey (FIRES), Franx et al. (2003) selected 14 candidate galaxies at $z > 2$ to a depth of $K_{AB} < 24.4$, of which 6 were spectroscopically confirmed (van Dokkum et al. 2003). Labbé et al. (2005) found that approximately 70% of DRGs are dusty star forming galaxies and the remaining 30% are passively evolved galaxies.

Recent work by van Dokkum et al. (2006) suggests that DRGs may be a significant constituent of the $z \sim 2 - 3$ universe in terms of stellar mass. Förster Schreiber et al. (2004) demonstrated that the average rest-frame optical colours of DRGs fall within the range covered by normal galaxies locally, unlike the Lyman-break galaxies (LBGs – Steidel et al. 1996) which are typically much bluer. Larger samples of DRGs covering a wide range in stellar mass are now required to fully understand the importance of this population. In particular, studies conducted so far have (by necessity) concentrated on DRGs selected over relatively small areas, and very little is known about the bright end of this population. In this paper we present a study of the first large sample of DRGs selected at bright IR magnitudes ($K_{AB} < 21$) in a contiguous area. We analyse the number counts and clustering and draw conclusions about their likely origin. Throughout this paper, we assume $\Omega_m = 0.3$, $\Omega_\Lambda = 0.7$ and $h = H_0/70 \text{ km s}^{-1} \text{ Mpc}^{-1}$.

* E-mail: Sebastien.Foucaud@nottingham.ac.uk

† Scottish Universities Physics Alliance

2 UKIDSS UDS EARLY DATA RELEASE

2.1 Survey and Early Data Release

The UKIRT Infrared Deep Sky Survey (UKIDSS – Lawrence et al. 2006)¹ is a next generation near-infrared sky survey which began observations in Spring 2005. The observations are carried out using the Wide-Field Camera (WFCAM – Casali et al., in preparation) at the 3.8-m United-Kingdom InfraRed Telescope (UKIRT). Comprising 5 sub-surveys, it will take 7 years to complete and will cover a range of areas and depths. For more details about UKIDSS and its photometric system refer to Lawrence et al. (2006) and Hewett et al. (2006). The deepest of these 5 sub-surveys, the Ultra-Deep Survey (UDS) aims to cover 0.8 deg^2 to a depth of $K_{AB} = 25.0$, $H_{AB} = 25.4$, $J_{AB} = 26.0$ (5σ , point-source). It is centred on the Subaru/XMM-Newton Deep Survey field (SXDS - Sekiguchi et al. 2005) at $02^{\text{h}}18^{\text{m}}00^{\text{s}}$, $-05^{\circ}00'00''$ (J2000).

Since February 10 2006, the UKIDSS Early Data Release (EDR) has been available to the ESO community². A full description of this data release is given in Dye et al. (2006). A detailed description of the data pipeline will appear in Irwin et al. (in preparation), and for the data archive in Hambly et al. (in preparation).

2.2 Image stacking and mosaics

The stacking of the UDS EDR data was performed by our team using a slightly different recipe to the standard UKIDSS pipeline. Given the (relatively) small size of the field, it is possible to create a full mosaic before extracting catalogues, rather than merge catalogues extracted from individual chips. Given the various jitter and offset sequences, this helps to optimise depth in overlap regions and to produce a more homogeneous final image.

Each observation block consists of a 4-pt mosaic to tile the 0.8 deg^2 field, producing 16 images each of approximately 15 minutes exposure (see Dye et al. 2006). Individual reduced frames for each observation block were extracted from the UKIDSS pipeline as the starting point for our final mosaiced stack (including astrometric and photometric solutions). We used the variance map produced by the pipeline to weight each frame before stacking and rescaled the pixel flux for each individual image using the pipeline zero-points. These images, together with their weight maps, were combined to produce the final stacks and their weight maps. This was carried out in a two-step process by using the `SWARP` software, an image resampling tool (Bertin et al. 2002). The final mosaiced images in the J - and K -band have the same pixel scale of $0.1342''$, with identical field centres and image scales to simplify catalogue extraction. The resulting images were visually inspected, and bad regions were masked out (areas around saturated stars, cosmetic problem areas, and low signal-to-noise borders). After masking, the usable area of this frame with uniform coverage is 0.62 deg^2 (2265.35 arcmin^2). We note that this is smaller than the expected 0.8 deg^2 mosaic since the UDS field centre was moved by approximately 8 arcmin shortly after UKIDSS observations began (to allow the use of brighter guide stars).

The image seeing as measured from the mosaiced images is $0.69''$ FWHM in K and $0.80''$ in J . By comparing bright stars from the entire UKIDSS survey with a comparable sample from 2MASS (Skrutskie et al. 2006), Dye et al. (2006) determined that the RMS accuracy of our astrometry is $\simeq 0.05''$ (i.e. less than one UDS

pixel) and for our photometry the RMS accuracy is $\lesssim 2\%$ (at bright magnitudes for point-like sources) in both J - and K - bands. From direct measurements of noise in a $2''$ aperture on the image we estimate 5σ limiting magnitudes of approximately $K_{AB} = 22.5$ and $J_{AB} = 22.5$.

2.3 Catalogue extraction

We found that the standard UKIDSS source detection software did not produce optimal catalogues for the UDS. This problem is being investigated for future releases of UKIDSS data. Meanwhile we have produced a much improved catalogue for the EDR by using the `SEXTRACTOR` software (Bertin & Arnouts 1996). The K -band image was used as the source detection image, since this is measurably deeper for most galaxy colours (as confirmed by a galaxy number counts analysis).

To optimise our catalogue extraction we performed a series of simulations to fine tune the `SEXTRACTOR` parameters. Artificial point-like sources were added to the real K -band image using the observed PSF with $\text{FWHM} = 0.69''$ (rejecting regions containing bright sources), and distributed with magnitudes in the range $14 < K_{AB} < 24$. From the resulting new image a catalogue was extracted using `SEXTRACTOR` and compared with the list of artificial source positions. This process was repeated 1000 times, and the resulting statistics allow us to estimate the catalogue completeness and the evolution of photometric errors. Using these simulations, `SEXTRACTOR` detection parameters were tuned to maximise completeness at the noise-determined 5σ depth of $K_{AB} = 22.5$, while simultaneously minimising the number of spurious sources. While formally optimised for point-like sources, we note that these were close to optimal when we generated artificial sources using a substantially more extended PSF ($\text{FWHM} = 1.2''$).

Assuming the background noise is symmetric about zero (early data do not suggest otherwise) we can estimate the spurious fraction by extracting sources from the inverted image and comparing with the number of sources extracted from the normal image. At our noise-determined magnitude limit of $K_{AB} = 22.5$ the fraction of spurious detections is found to be less than 1%, while the completeness level is above 70% (for point sources).

Using these parameters, we extracted 78709 sources over 0.62 deg^2 from the image, of which 34098 were determined to be unsaturated, unmasked and from regions of uniform coverage to $K_{AB} < 22.5$. These form the basis of the analysis outlined below.

3 SELECTION AND NUMBER COUNTS

3.1 Selection of DRGs

From the catalogue described above we selected objects using the $(J-K)_{AB} > 1.3$ criteria ($2''$ aperture colour). A visual inspection of each source was then required to remove spurious detections, which at these extreme colours was found to be a relatively large fraction ($\sim 20\%$). The majority are caused by diffraction spikes and cross-talk images (Dye et al. 2006) and are easy to identify and reject. This leaves 369 DRGs at $K_{AB} < 21.2$, which represents the largest sample selected over a contiguous area. Figure 1 shows the $(J-K)$ colour of these galaxies versus K -band magnitude. The object shown by a star was classified as a point-like source in our global catalogue, and is confirmed to be a star after visual inspection. This object is under further investigation.

¹ <http://www.ukidss.org>

² <http://surveys.roe.ac.uk/wsa>

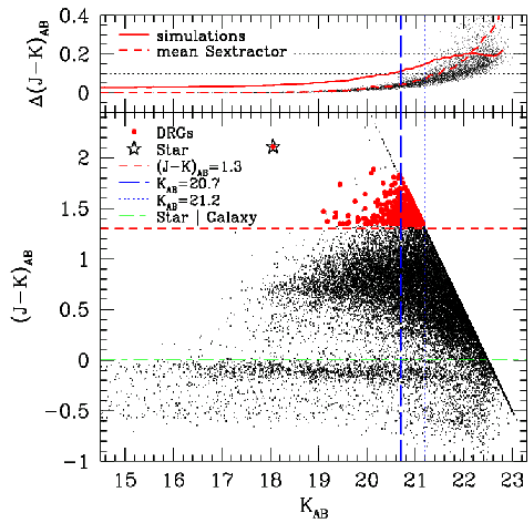


Figure 1. *Lower panel:* $(J - K)_{AB}$ against K_{AB} for galaxies with $K_{AB} < 22.5$ in the UDS field. Small points represent the full population of K-band selected objects, while larger points are those selected with $(J - K)_{AB} > 1.3$ (and visually confirmed). The $(J - K)_{AB} > 1.3$ criteria, the magnitude limit at $K_{AB} = 21.2$ and the magnitude completeness at $K_{AB} = 20.7$ are highlighted, as is the crude boundary between galaxies and the stellar locus at $(J - K)_{AB} = 0$. *Upper panel:* Errors as derived by `SExtractor` on the $(J - K)_{AB}$ colours (for display purposes only 1/5th of the points are shown). Mean values are also displayed, as are errors derived from simulations.

3.2 Photometric errors and contamination of DRG sample

Since our sample is based on $(J - K)$ colour selection it is vital to carefully consider the effects of photometric errors. Since most galaxies show substantially bluer colours (Figure 1) we can expect the number density of DRGs to be artificially boosted at fainter magnitudes, as errors push objects above the $(J - K)_{AB} > 1.3$ selection boundary. As a lower limit to this contamination we can use the photometric errors derived from `SExtractor`, and these are shown as a function of magnitude in Figure 1. Our experience suggests that analytically-determined errors from `SExtractor` are likely to be underestimates, so we also use the mean photometric errors obtained from the simulations described in section 2.3.

We used both sets of errors to estimate the contamination by randomising the real galaxy catalogue using Monte-Carlo simulations. For each object in our full catalogue, we allow the $(J - K)$ colour to vary assuming a Gaussian distribution with a standard deviation corresponding to the chosen photometric error. We then re-select our catalogue using the $(J - K)_{AB} > 1.3$ criteria, and repeat this process 1000 times. If the photometric errors are correct this should provide an approximate upper limit on contamination, since we are randomising the observed galaxy catalogue (which already suffers from the effects of photometric errors).

Defining the contamination fraction from the number of objects scattered into our selection boundary minus those which are scattered out, the `SExtractor` errors yield contamination fractions of $12.3 \pm 2.4\%$ at the limiting magnitude of $K_{AB} < 21.2$, falling to $3.6 \pm 2.2\%$ at $K_{AB} < 20.7$ (the estimated completeness limit; see Section 3.3). Using our simulated source errors, the contamination is substantially higher, reaching $46.0 \pm 3.8\%$ at $K_{AB} < 21.2$, falling to $16.8 \pm 3.6\%$ at $K_{AB} < 20.7$.

Based on these values we conclude that our number counts and

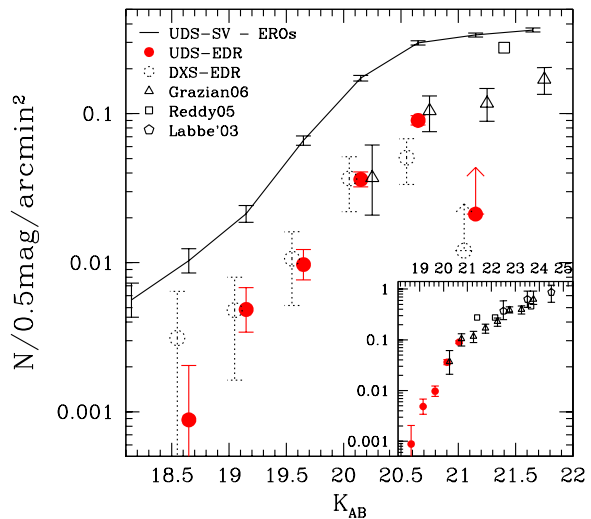


Figure 2. K -band differential number counts for our sample of DRGs. The errorbars plotted are computed from poissonian small number statistics (Gehrels 1986). For comparison, we have overplotted the number counts for DRGs derived from the DXS EDR survey, with errors representing the field-to-field variance (see section 3.4 – these points are slightly shifted for display purposes), and from the literature from fainter samples (Labbé et al. 2003; Reddy et al. 2005; Grazian et al. 2006). EROs number counts from the UDS/DXS SV sample are shown as well, for comparison. The plot inset shows number counts over a larger magnitude range.

clustering measurements are reasonably robust at $K_{AB} < 20.7$, but will become increasingly unreliable at fainter magnitudes. We will therefore adopt a limit of $K_{AB} = 20.7$ for further study, which produces a sample of 239 DRGs.

3.3 Number counts of DRGs

Figure 2 shows the K -band differential number counts of our sample of DRGs. The number counts indicate that our sample is only complete up to approximately $K_{AB} \simeq 20.7$, after which the counts are clearly dropping. This defines our estimated completeness limit, as used in our simulations in section 3.2. Our simulations suggest that the contamination due to photometric errors will be at most 16% at $K_{AB} < 20.7$, so we conclude that the dominant source of error in our number counts will be Poisson counting errors (plotted) and cosmic variance (discussed in section 3.4).

At bright magnitudes (e.g. $K_{AB} < 20$) our UKIDSS data are entirely unique, and no studies exist in the literature for comparison. At fainter magnitudes, our counts are in very good agreement with the DRG counts from the Grazian et al. (2006) sample. Combining literature data with the present work we can examine the global shape of the DRG number counts over a very wide dynamic range ($18.5 < K_{AB} < 25.0$). This strongly suggests a break feature in the slope at $K_{AB} \sim 20.5$ which is an effect already seen in the global K-band number counts (e.g. Gardner et al. 1993).

Comparing with Extremely Red Objects (EROs) and global K -band number counts, e.g. as derived from the UDS/DXS SV sample (Lawrence et al. 2006), we note that the projected density of DRGs is approximately 10 times lower than EROs, and approximately 100 times lower than the global galaxy counts at a given magnitude.

3.4 Cosmic variance

As a simple test of cosmic variance, and to investigate whether the UDS is an unusual field, we used the data available from the UKIDSS Deep Extragalactic Survey (DXS) to perform a comparison study of DRG number counts. The DXS is the other deep extragalactic component of UKIDSS (Lawrence et al. 2006), consisting of 4 fields with a 7-year goal of observing 35 deg² to depths of $K_{AB} = 22.7$ and $J_{AB} = 23.2$. In the UKIDSS EDR and SV (Science Verification), 8.3 deg² were observed in K and 3.3 deg² in J . While exposure times are similar to the UDS EDR, the observing conditions are generally poorer (typical seeing is around 1.0 – 1.2"). Direct comparison is also complicated by the slightly different source extraction methods used by the DXS.

In order to select DRGs from those fields, we used the only areas of 3 fields observed in both J - and K -bands : XMM-LSS (02^h27^m, –04°40'), Elais-N1 (16^h00^m, +57°00') and VIMOS-4 (22^h17^m, +00°24'), covering ~ 2900 arcmin², ~ 4500 arcmin² and ~ 2900 arcmin² respectively. We applied the same selection method described in section 3.1, except that we did not visually inspect the samples. This selects 659 objects in the XMM-LSS field, 350 in Elais-N1 and 514 in VIMOS-4. We derived a median surface density of $n = 0.176 \pm 0.075$ arcmin⁻² at $K_{AB} = 21.2$. This is in good agreement with the density measured in the UDS.

Based on our experience with the UDS data, we estimate that approximately 20% of DRGs from the DXS are likely to be spurious (see section 3.1). We also estimate that the number of DRGs is likely to be artificially boosted due to photometric errors (section 3.2). Since these errors are smaller than the errors in the DXS counts, for simplicity we opt not to make these corrections in our comparison with the UDS.

The resulting median counts from the 3 DXS samples are overplotted in figure 2, with errors representing the field-to-field variance. The agreement with UDS is very good. Although the contamination and spurious fraction have not been corrected for rigorously, this crude comparison suggests that the density of DRGs is stable and broadly consistent between fields.

4 THE CLUSTERING OF DRGS

4.1 Angular clustering

In Figure 3, we display the distribution of our sample of DRGs on the sky. Visually the DRGs appear strongly clustered. As a more quantitative measure, we evaluate the 2-point angular correlation function, cutting our sample at $K_{AB} = 20.7$ as before.

To measure the angular correlation function $\omega(\theta)$ and estimate the related poissonian errors we used the Landy & Szalay (1993) estimators. Figure 4 shows the correlation function derived from our DRG sample. The best fit for the angular correlation is assumed to be a power-law as (Groth & Peebles 1977):

$$\omega(\theta) = A_\omega(\theta^{-\delta} - C_\delta)$$

with the amplitude at 1 degree $A_\omega = 3.13^{+2.13}_{-1.31} \times 10^{-3}$, the slope $\delta = 1.0 \pm 0.1$, and the integral constraint due to the limited area of the survey $C_\delta = 3.71$ (determined over the unmasked area).

As shown in figure 4, by comparing with various measurements from Kong et al. (2006) at the same magnitude limit of $K_{AB} < 20.7$, the amplitude of the DRG sample is ~ 5 times higher than that of field galaxies but perhaps a factor of ~ 2 lower than EROs and BzK-selected galaxies. Interestingly, our derived clustering amplitude is notably higher than recent measurements

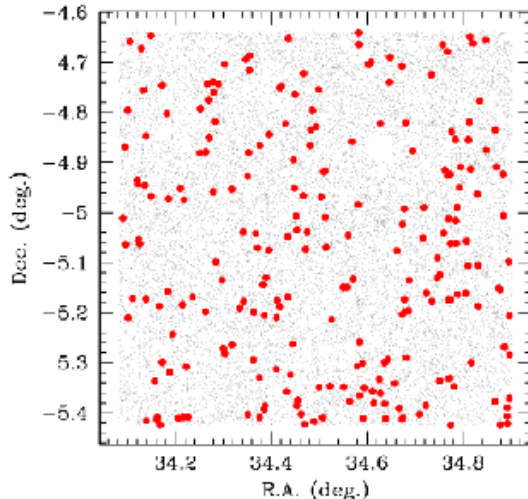


Figure 3. Distribution of our sample of DRGs on the sky, providing a visual impression of the large scale structure. Small dots represent the full K-band galaxy sample, while larger symbols are the DRGs with $K_{AB} < 20.7$.

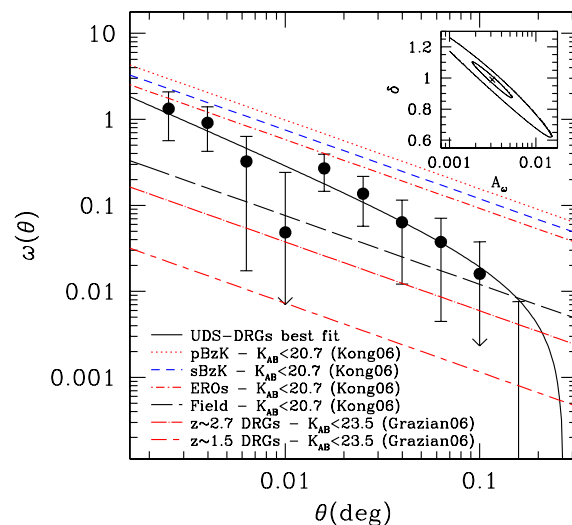


Figure 4. 2-point angular correlation function determined for our sample of DRGs with $K_{AB} < 20.7$ with its fitted power-law. The plot inset presents the χ^2 minimisation to estimate the best-fitted values of A_ω and δ , with contours showing 1 σ and 3 σ confidence levels. For comparison, measurements from the literature for different samples are overplotted, assuming a slope of $\delta = 0.8$ (Kong et al. 2006; Grazian et al. 2006).

for DRGs obtained by Grazian et al. (2006), who evaluated $\omega(\theta)$ for samples of DRGs at low-redshift ($z \sim 1.5$) and high redshift ($z \sim 2.7$). If we make the (untested) assumption that our galaxies sample similar redshifts to the $z \sim 1.5$ subset from Grazian et al. (2006) then we may interpret our higher amplitude as evidence for mass/luminosity segregation (e.g. Pollo et al. 2006), since we will be sampling the brighter end of the luminosity function.

As discussed in Section 3.3, the contamination of our DRG sample by bluer galaxies due to photometric errors is likely to be modest ($< 16\%$). This will dilute the DRG angular correlation function, but is unlikely to be a major effect.

4.2 Spatial correlation lengths and biasing

In order to compare the clustering of galaxy populations at different redshifts we must derive spatial correlation measurements. If we assume a redshift distribution for our sample we can derive the correlation length using the relativistic Limber equation (Magliocchetti & Maddox 1999), and in addition derive a linear bias estimation (Magliocchetti et al. 2000). The difficulty here is to have a realistic estimation of the redshift distribution of our sample. While Franx et al. (2003) have designed the $(J - K)_{AB} > 1.3$ criteria to select $z > 2$ galaxies, Grazian et al. (2006) and Conselice et al. (2006) have shown that the redshift distribution is broad, and the fraction of $z < 2$ galaxies increases dramatically at brighter magnitudes.

As a preliminary investigation we assume a Gaussian form for the redshift distribution, fixing the mean and standard deviation to match recent studies of fainter DRGs. The correlation length can then be evaluated if we fix the slope of the correlation function to $\gamma = 1 + \delta = 2.0$. In the DRG sample of Grazian et al. (2006), a mean redshift of $\bar{z} = 1.5$ was found at a limit of $K_{AB} < 22.0$. Using this mean redshift with $\sigma = 0.5$ (broadly matching their distribution) we determine $r_0 = 14.1^{+4.8}_{-2.9} h^{-1} \text{Mpc}$ and $b = 4.8^{+1.7}_{-1.1}$ for our DRGs. Conselice et al. (2006) suggest that very bright DRGs lie at even lower redshifts. If we adopt the approximate redshift distribution of their spectroscopic sample (with $\bar{z} = 1.1$ and $\sigma = 0.3$), we derive $r_0 = 11.6^{+4.0}_{-2.4} h^{-1} \text{Mpc}$ and $b = 4.3^{+1.5}_{-0.9}$.

Grazian et al. (2006) also split their sample according to redshift, and found $r_0 = 7.4^{+3.5}_{-4.9} h^{-1} \text{Mpc}$ for DRGs at $1 < z < 2$ with $K_{AB} < 22$. Our sample is substantially brighter, so our somewhat larger correlation length could be interpreted as evidence for luminosity segregation, e.g. we may be sampling more luminous galaxies which are more strongly biased (Pollo et al. 2006).

As shown in figure 4, our measurement is comparable to the clustering of EROs or BzK selected galaxies at the same limiting magnitude, which are likely to sample a similar redshift distribution to our DRGs, and hence show similar correlation lengths. Overzier et al. (2003) compared the clustering of EROs with predictions of Dark Matter halo models. Adopting the same technique, we can infer that bright DRGs are likely to be hosted by very massive dark matter halos (possibly $M > 10^{14} M_{\odot}$), consistent with the potential progenitors of present-day $L \gtrsim L_*$ elliptical galaxies.

5 SUMMARY

We have extracted a large sample of bright Distant Red Galaxies from the UKIDSS UDS EDR. Our catalogue contains 369 DRGs to a limiting magnitude of $K_{AB} = 21.2$, extracted over an area of 0.62 deg^2 . The fainter $K_{AB} > 20.0$ number counts are in good agreement with previous estimates, while at brighter magnitudes the sample is unique. Using simulations we determined that contamination due to photometric errors is below $\sim 16\%$ at an approximate completeness limit of $K_{AB} < 20.7$.

From this sample we extracted a sub-sample of 239 bright DRGs to a limit of $K_{AB} = 20.7$. These bright DRGs appear highly clustered, and we determine a correlation length of $r_0 \simeq 12 h^{-1} \text{Mpc}$ and a bias measurement $b \simeq 4.5$ if we assume the sample lies at a mean redshift of $\bar{z} = 1.1$ with a standard deviation of $\sigma = 0.3$ (consistent with recent studies at similar depths – Conselice et al. 2006). They appear more clustered than fainter samples of DRGs derived at these redshifts, which may be evidence for luminosity segregation, in agreement with biased galaxy formation scenarios.

ACKNOWLEDGEMENTS

The authors would like to thank Stephen Warren and Stephen Searjeant for their useful comments. This work is based entirely on data obtained as part of the UKIRT Infrared Deep Sky Survey. We are grateful to the staff at UKIRT for making these observations possible. We also acknowledge the Cambridge Astronomical Survey Unit and the Wide Field Astronomy Unit in Edinburgh for processing the UKIDSS data. SF, CS and MC acknowledge funding from PPARC. OA, IS and RJM acknowledge the support of the Royal Society.

REFERENCES

- Bertin, E. & Arnouts, S. 1996, *A&A*, 117, 393
 Bertin, E., Mellier, Y., Radovich, M., et al. 2002, in *ASP Conf. Ser. 281: Astronomical Data Analysis Software and Systems XI*, ed. D. A. Bohlender, D. Durand, & T. H. Handley, 228–+
 Conselice, C. J., Newman, J. A., Georgakakis, A., et al. 2006, *ApJ*, *submitted*
 Dye, S., Warren, S. J., Hambly, N. C., et al. 2006, *MNRAS*, *submitted* – astro-ph/0603608
 Förster Schreiber, N. M., van Dokkum, P. G., Franx, M., et al. 2004, *ApJ*, 616, 40
 Franx, M., Labbé, I., Rudnick, G., et al. 2003, *ApJ*, 587, L79
 Gardner, J. P., Cowie, L. L., & Wainscoat, R. J. 1993, *ApJ*, 415, L9
 Gehrels, N. 1986, *ApJ*, 303, 336
 Grazian, A., Fontana, A., Moscardini, L., et al. 2006, *A&A*, *submitted* – astro-ph/0603095
 Groth, E. J. & Peebles, P. J. E. 1977, *ApJ*, 217, 385
 Hewett, P. C., Warren, S. J., Leggett, S. K., & Hodgkin, S. T. 2006, *MNRAS*, *in press* – astro-ph/0601592
 Kong, X., Daddi, E., Arimoto, N., et al. 2006, *ApJ*, 638, 72
 Labbé, I., Franx, M., Rudnick, G., et al. 2003, *AJ*, 125, 1107
 Labbé, I., Huang, J., Franx, M., et al. 2005, *ApJ*, 624, L81
 Landy, S. D. & Szalay, A. S. 1993, *ApJ*, 412, 64
 Lawrence, A., Warren, S. J., Almaini, O., et al. 2006, *MNRAS*, *submitted* – astro-ph/0604426
 Magliocchetti, M., Bagla, J. S., Maddox, S. J., & Lahav, O. 2000, *MNRAS*, 314, 546
 Magliocchetti, M. & Maddox, S. J. 1999, *MNRAS*, 306, 988
 Overzier, R. A., Röttgering, H. J. A., Rengelink, R. B., & Wilman, R. J. 2003, *A&A*, 405, 53
 Pollo, A., Guzzo, L., Le Fèvre, O., et al. 2006, *A&A*, 451, 409
 Reddy, N. A., Erb, D. K., Steidel, C. C., et al. 2005, *ApJ*, 633, 748
 Sekiguchi, K., Akiyama, M., Furusawa, H., et al. 2005, in *Multiwavelength Mapping of Galaxy Formation and Evolution*, ed. R. Bender & A. Renzini, 82–+
 Skrutskie, M. F., Cutri, R. M., Stiening, R., et al. 2006, *AJ*, 131, 1163
 Steidel, C. C., Giavalisco, M., Dickinson, M., & Adelberger, K. L. 1996, *AJ*, 112, 352+
 van Dokkum, P. G., Förster Schreiber, N. M., Franx, M., et al. 2003, *ApJ*, 587, L83
 van Dokkum, P. G., Quadri, R., Marchesini, D., et al. 2006, *ApJ*, 638, L59